

**Observational evidence for the accretion of low-metallicity
gas onto the Milky Way:
metallicity, physical conditions and distance limit for HVC
complex C**

B.P. Wakker, J.C. Howk, B.D. Savage, S.L. Tufte, R.J. Reynolds

Department of Astronomy, University of Wisconsin, Madison, WI 53706

H. van Woerden, U.J. Schwarz

Kapteyn Institute, Rijks Universiteit Groningen, The Netherlands

R.F. Peletier

University of Durham, UK

Abstract. We present observations of the (field of the) Seyfert galaxy Mark 290, which probes the high-velocity cloud (HVC) complex C, one of the largest HVCs (Wakker & van Woerden 1991). We find that this object has a metallicity of $0.094 \pm 0.020^{+0.022}_{-0.019}$ times solar. We determine a lower limit to its distance of 5 kpc ($z > 3.5$ kpc). If the gas is in thermal equilibrium with a hot halo, then it is also likely that $D < 30$ kpc, putting the HVC in the Galactic Halo, as was the case for HVC complex A (for which $z = 2.5\text{--}7$ kpc; van Woerden et al. 1998).

We find that, on this sightline, H^+ represents $23 \pm 10\%$ of the hydrogen in the HVC. The total gaseous mass is $2.0 \times 10^6 (D/5 \text{ kpc})^2 M_\odot$ and, depending on whether the space velocity is completely radial or vertical, the HVC represents a downward mass flux of $\sim 0.036\text{--}0.083 (D/5 \text{ kpc}) M_\odot \text{ yr}^{-1}$, or $\sim 2.9\text{--}6.7 \times 10^{-3} (D/5 \text{ kpc})^{-1} M_\odot \text{ yr}^{-1} \text{ kpc}^{-2}$.

The low metallicity and large mass suggest that complex C is unlikely to be part of a Galactic Fountain, but rather represents accreting low-metallicity material. It may be a present-day analogue of the damped $\text{Ly}\alpha$ absorbers seen in QSO spectra. Our abundance result provides the first direct observational evidence for the infall of low-metallicity gas on the Milky Way, required in models of galactic chemical evolution.

It remains to be seen whether ultimately complex C is a remnant of the formation of the Milky Way (Oort 1970), a gas cloud orbiting the Galaxy (Kerr & Sullivan 1969), a Local Group object (Verschuur 1969, Blitz et al. 1996), the result of tidal interactions between the Magellanic System and the Galaxy >3 Gyr ago (an "Old Magellanic Stream"; Toomre, quoted in Kerr & Sullivan 1969), or was formed when hot, ionized intergalactic gas was compressed by the motion of the Milky Way (Silk et al. 1987).

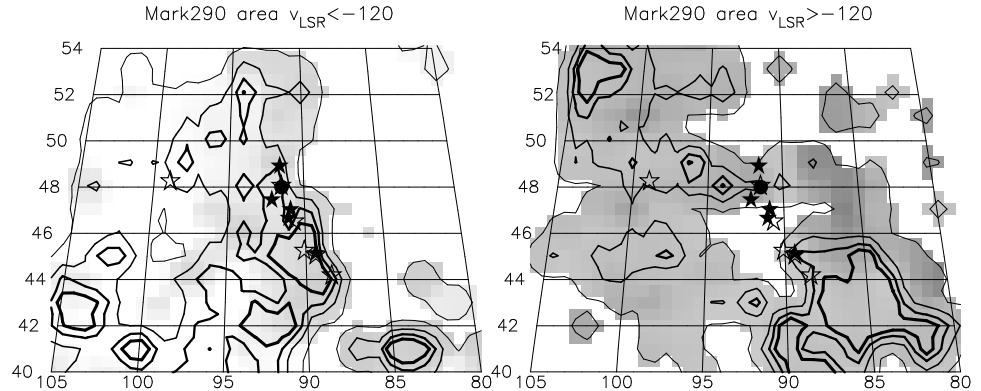


Figure 1. HI column density maps of part of complex C (data from Hulsbosch & Wakker 1988). Brightness temperature contour levels are 0.05 K and 25%, 50%, 75% and 100% of the peak value of the concentration nearest Mark 290. Filled symbols indicate probe stars whose spectrum is included in Fig. 4. Larger symbols are for more distant stars. Mark 290 is shown by the filled circle.

1. Introduction

In this contribution we describe results based on many observations of HVC complex C toward and near the Seyfert galaxy Markarian 290 ($V=14.96$, $z=0.030$). Figure 1 shows the large-scale HI structure of the HVC this region. Among all known extra-galactic probes of complex C, Mark 290 is the most favorable in terms of the expected strength of absorption lines.

In Sect. 2 we discuss recent optical absorption-line data that allow us to set a lower limit to the distance of the HVC. Sect. 3 describes the SII absorption-line data, and in Sect. 4 we present data on optical and radio emission lines. Sect. 5 describes a method for deriving an ionization-corrected metallicity, ionization fraction, density and pressure for the cloud. This method is applied in Sect. 6, and the implications are discussed in Sect. 7.

2. Distance limit

Using the William Herschel Telescope (WHT) at La Palma, and the Utrecht Echelle Spectrograph (UES), we observed CaII H+K spectra of 12 stars in the region around Mark 290, at 6 km/s resolution. The stars were selected from a list of blue stars by Beers et al. (1996, and references therein). We chose stars that were classified as Blue Horizontal Branch in low-resolution spectra; follow-up spectroscopy confirms this for 80% of such stars (Beers et al. 1992). For these BHB candidates, a rough distance estimate can be made by assuming $B-V=0.05$, and inserting this into the $B-V$ vs M_V relation of Preston et al. (1991). This gives $M_V=0.86$. Averaged over all possible colors, the full range is ± 0.25 mag, so we calculated a probable distance range using $M_V=0.61$ and

1.11. An extinction correction of ~ 0.1 mag was applied, using A_V based on the map of Lucke (1978).

For the most distant stars the spectra are of relatively low quality, while for some others stellar lines interfere with the detection of interstellar features. Figure 2 shows five of the best CaII K spectra, from which we can set tentative limits on the strength of the Ca K absorption. The expected equivalent widths can be derived from the CaII/HI ratio of $29 \pm 2 \times 10^{-9}$ found toward Mark 290 by Wakker et al. (1996), combined with the N(HI) in the direction of the star.

The estimated detection limit on the CaII K absorption associated with the HVC is always lower than the expected value. Since for three of the stars we estimate $D \sim 5$ kpc, we conclude that the distance of complex C is probably > 5 kpc. However, there are three caveats.

- a) The HI column densities are based on a $9'$ beam, but considerable variations at arcminute scales are possible (Wakker & Schwarz 1991). Only a ratio (expected/detection-limit) > 5 allows a safe conclusion.
- b) The equivalent width limits are still preliminary.
- c) The stellar distances need to be improved using spectroscopy.

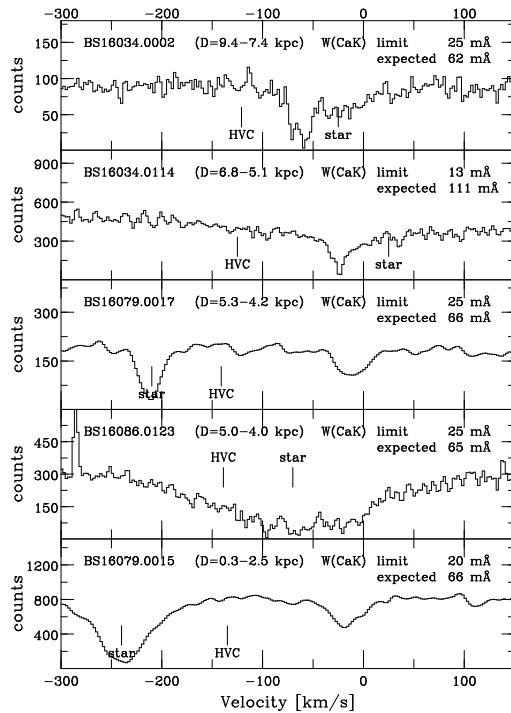


Figure 2. CaII K spectra of five stars projected on complex C. The range of possible distances is shown, as are the detection limit and expected equivalent width. The velocities of the HVC (from an Effelsberg spectrum) and the star (from stellar features elsewhere in the spectrum) are indicated by the lines labeled "HVC" and "star".

3. Observations - SII absorption

We observed SII absorption with the G140M grating of the Goddard High Resolution Spectrograph (GHRS) on the Hubble Space Telescope (HST). Sulphur is one of a few elements not depleted onto dust in the ISM, and S^+ is the dominant ionization stage in neutral gas (Savage & Sembach 1996). Thus, $N(S^+)$ allows a good measure of the intrinsic metallicity of an HI cloud. Among all similar ions, the SII $\lambda\lambda 1250, 1253, 1259$ lines are the easiest to observe.

The integration time was 90 minutes, the resolution 15 km/s. The SII lines occur on top of strong $\text{Ly}\alpha$ emission associated with Mark 290, which increases the S/N ratio in the continuum at 1253 Å to 25, whereas it is only 12 at 1259 Å. The $\lambda 1250$ absorption is hidden by absorption associated with Mark 290.

The left top two panels of Fig. 3 show the spectra after continuum normalization. The vertical lines correspond to zero velocity relative to the LSR and to the two components observed at -138 and -115 km/s in HI (Wakker et al. 1996 and Fig. 3). The HVC component at -138 km/s is clearly seen in both SII lines, but the -115 km/s component is missing, although a component at -110 km/s may be present in the CaII spectrum. This component may be missing due to a combination of factors. First, it is wider (FWHM 31 km/s vs 21 km/s). Second, in the 9' beam it has a factor 1.6 lower HI column density. Third, fine structure in the emission may decrease the HI column density even further; this is especially so for the -115 km/s component as Mark 290 is near the edge of the -115 km/s core (see Fig. 1). In combination these may cause the SII peak optical depth to become too low to detect the line with the current S/N ratio.

Fitting the absorption lines between -165 and -125 km/s gives equivalent widths for the $\lambda 1253$ and $\lambda 1259$ lines of 20.3 ± 3.4 and 32.7 ± 5.2 mÅ. Assuming no saturation and using f -values from Verner et al. (1994), these correspond to column densities of $1.50 \pm 0.25 \times 10^{14}$ and $1.63 \pm 0.30 \times 10^{14}$ cm $^{-2}$. The average, weighted by the S/N in the continuum, is $1.54 \pm 0.27 \times 10^{14}$. Half of this error is associated with the placement of the continuum.

These absorption lines are unresolved, but likely to be unsaturated. We base this conclusion on three lines of evidence. First, the CaII lines toward Mark 290 were resolved by Wakker et al. (1996) (FWHM 14 km/s at 6 km/s resolution), so the expected linewidth for SII is 16 km/s; an equivalent width of 20.3 ± 3.4 mÅ would then give a column density of $1.6 \pm 0.3 \times 10^{14}$ cm $^{-2}$, in agreement with the value derived above. Second, the observed ratio of equivalent widths is 1.6 ± 0.4 , which is compatible with the expected ratio of 1.51. Third, for gas at temperature ~ 7000 K (see Sect. 6), the thermal b -value for S is 1.9 km/s; the observed equivalent width then corresponds to an optical depth of 3.5 for the $\lambda 1253$ line. However, this predicts an equivalent width of 23.2 mÅ for the $\lambda 1259$ line, which is outside the error limit. If $W(1259)$ were $1.51 \times 20.3 - 1\sigma = 25.5$ mÅ, then for $W(1253)$ to be 20.3 mÅ one requires $b = 2.9$ km/s with $\tau = 1.5$ and 2.25 for the $\lambda 1253$ and 1259 lines, respectively. This corresponds to a column density of 2.25×10^{14} cm $^{-2}$, just 2.5σ higher than the preferred value above.

The SII column density likely represents the total S column density. In the ISM sulphur will exist as S^+ and either S^0 or S^{+2} . S^0 has an ionization potential of 10.4 eV, and thus is easily ionized by the ambient radiation field. We do not

detect $\text{SI}\lambda 1262.86$, setting a limit of $\text{N}(\text{S}^0) < 2.6 \times 10^{14} \text{ cm}^{-2}$, or $\text{N}(\text{S}^+)/\text{N}(\text{S}^++\text{S}^0) > 0.37$. S^+ has an ionization potential of 23.3 eV. If we assume that inside the part of the cloud where H is fully ionized all S is S^{+2} (which would imply that there is no [SII] emission), then, since we always find $\text{N}(\text{H}^+) < \text{N}(\text{HI})$ (Sect. 6), we conclude that $\text{N}(\text{S}^+)/\text{N}(\text{S}^++\text{S}^{+2}) > 0.5$. In low-velocity neutral gas this ratio is always observed to be > 0.9 .

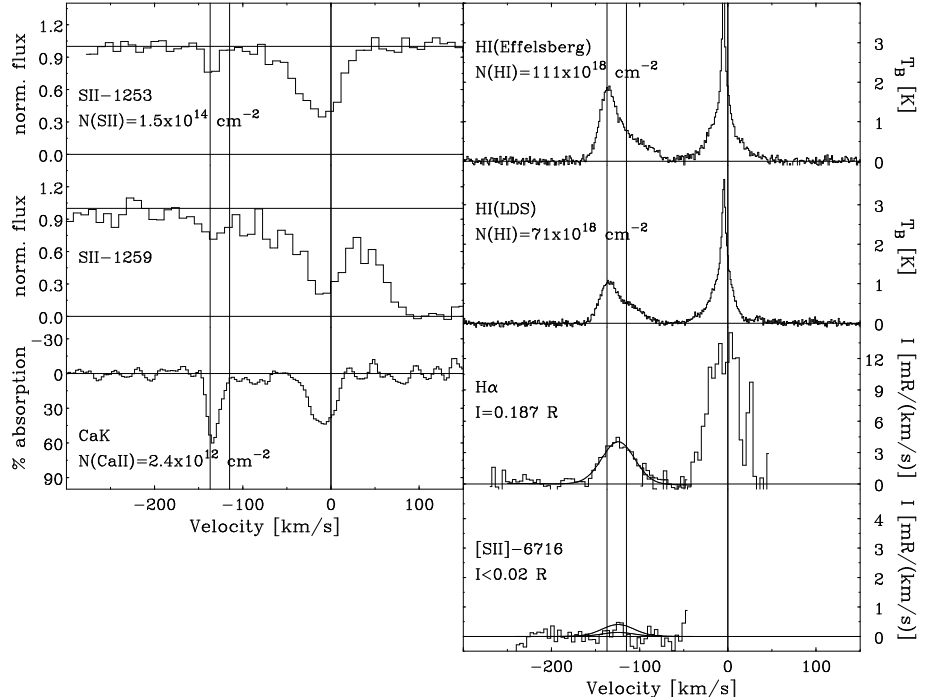


Figure 3. Spectra using Mark 290 as a light bulb or centered on Mark 290, aligned in velocity. The labels give the spectral line and the resulting measured column density or intensity for the HVC. For the [SII] emission spectrum (WHAM data) two curves are drawn, corresponding to 1/10th and 1/30th the $\text{H}\alpha$ intensity.

4. Observations - emission lines

To determine a metallicity from the SII column density, HI data with the highest-possible resolution are required (see discussion in Wakker & van Woerden 1997). We have data from Westerbork at 1 arcmin resolution, but these have not yet been analyzed. Until then we will use a 9 arcmin resolution Effelsberg spectrum from Wakker et al. (1996). This spectrum is shown in Fig. 3. There are two components, at -138 and -115 km/s, with $\text{N}(\text{HI}) = 68 \pm 3$ and $43 \pm 7 \times 10^{18} \text{ cm}^{-2}$.

Using the Wisconsin $\text{H}\alpha$ Mapper (WHAM, Reynolds et al. 1998), we observed the $\text{H}\alpha$ and [SII] $\lambda 6716$ emission in a one-degree diameter field centered on Mark 290. $\text{H}\alpha$ emission is clearly detected ($I_R = 0.187 \pm 0.010$ R; where 1

Rayleigh is $10^6/4\pi \text{ ph cm}^{-2} \text{ s}^{-1} \text{ sr}^{-1}$). The spectrum in Fig. 3 has 12 km/s resolution and is a combination of integrations of 20 min for $v < -50 \text{ km/s}$ and 30 sec for $v > -100 \text{ km/s}$. Most of the “noise” at lower velocities is fixed-pattern-noise.

[SII] emission is not detected, although the $1-\sigma$ noise level is 0.006 R. Thus, we can set a $3-\sigma$ limit of <0.1 for the ratio of $\text{H}\alpha$ and [SII] intensities. WHAM usually sees a ratio of ~ 0.3 .

To compare the $\text{H}\alpha$ and HI, an HI spectrum of the full 1-degree WHAM field is required, which was created from the Leiden-Dwingeloo survey (Hartmann & Burton 1997) by averaging the 4 spectra inside the WHAM beam. This spectrum is also shown in Fig. 3 and gives column densities of 40.0 ± 2.7 and $30.6 \pm 2.9 \times 10^{18} \text{ cm}^{-2}$ for the two HI components. The apparent velocity shift between $\text{H}\alpha$ and HI is probably due to a different intensity ratio between the two high-velocity components and the lower velocity resolution of the $\text{H}\alpha$ data.

5. Physical conditions - theory

We now show how the HI, $\text{H}\alpha$, SII absorption and [SII] emission data can be combined to derive an ionization-corrected S abundance (A_S), temperature (T), central density (n_o) and total ionization fraction (X). We only need to assume a distance and a particular geometry, i.e. a density and ionization structure.

We define the density structure in the sightline as $n(z)$ and the ionization structure as $x(z)$, the ratio of ionized to total H (assuming $n(\text{H}_2)=0$). The “standard” model consists of a cloud with diameter L with a fully neutral core with diameter l and a fully ionized envelope with constant density [$n(z) = n_o$ for $z < L/2$]. Figure 1 shows that the FWHM angular diameter of the cloud, α , is 2 ± 0.2 degrees; the linear diameter L is the product of α and the distance (D).

To investigate the effects of different geometries we go one step beyond this “standard model” and allow for a gaussian density distribution [$n(z) = n_o \exp(-4 \ln 2 z^2/L^2)$] and for the ionization fraction in the core and envelope to be different from 0 or 1 [$x(z)=x_n$ for $z < l$; $x(z)=x_i$ for $z > l$]. We then need the following integrals:

$$\begin{aligned} \int_{-\infty}^{\infty} x(z)n(z)dz &= an_o L [(1-r)x_n + rx_i] = \mathcal{F}_1 n_o L \\ \int_{-\infty}^{\infty} x(z)n^2(z)dz &= \frac{a}{b} n_o^2 L [(1-r)x_n + rx_i] = \mathcal{F}_2 n_o^2 L \\ \int_{-\infty}^{\infty} x^2(z)n^2(z)dz &= \frac{a}{b} n_o^2 L [(1-r)x_n^2 + rx_i^2] = \mathcal{F}_3 n_o^2 L, \end{aligned}$$

where for a gaussian $r=1 - \text{erf}(\sqrt{4 \ln 2} l/L)$, $a=\sqrt{\pi/4 \ln 2}$, $b=\sqrt{2}$, and for a uniform density distribution $r=1-(2l/L)$, $a=1$, $b=1$. For the “standard model”, all three \mathcal{F} values reduce to the “filling factor”.

The definition of $\text{H}\alpha$ emission measure and its relation to observables are:

$$\text{EM} = \int n_e(z) n(\text{H}^+)(z) dz = 2.75 T_4^{0.924} I_R \text{ cm}^{-6} \text{ pc},$$

with T_4 the temperature in units of 10000 K, and I_R the $\text{H}\alpha$ intensity in Rayleigh.

For a cloud with substantial ionization, but still containing neutral gas, most electrons will come from H, so that $n_e = \epsilon n(H^+)$, with $\epsilon > 1$. The first ionization potential of He is 24.6 eV, so He will not give a substantial contribution in mostly neutral gas. Because of their much lower abundances all other elements combined contribute at most a few percent, even if fully ionized. Thus, we have the following expressions for the H^+ and HI column density and the $H\alpha$ intensity in terms of the structure parameters:

$$\begin{aligned} N(H^+) &= \int_{-\infty}^{\infty} x(z)n(z)dz = \mathcal{F}_1 n_o L \\ N(HI) &= \int_{-\infty}^{\infty} (1 - x(z))n(z)dz = (a - \mathcal{F}_1) n_o L \\ 2.75 T_4^{0.924} I_R &= EM = \int_{-\infty}^{\infty} \epsilon x^2(z)n^2(z)dz = \epsilon \mathcal{F}_3 n_o^2 L. \end{aligned}$$

To convert the observable (intensity) into the emission measure, we need to know the gas temperature. This can be found by combining the S^+ emission and absorption data. The ratio of S^+ and H^+ emissivity is:

$$\frac{\epsilon(SII)}{\epsilon(HII)} = 7.73 \times 10^5 T_4^{0.424} \exp\left(\frac{-2.14}{T_4}\right) \left(\frac{n_{S^+}}{n_{H^+}}\right) = F(T) \left(\frac{n_{S^+}}{n_{H^+}}\right).$$

The density of S^+ is $n(S^+)(z) = A_S n(z)$, with A_S the S^+ abundance. Thus, locally, the emissivity ratio is some constant times the density ratio. If we assume that S^+ emission occurs only in the part of the cloud where electrons are present, and if we assume a constant temperature, then the intensity ratio is:

$$E = \frac{I(SII)}{I(HII)} = F(T) \frac{\int n_e n_S dz}{\int n_e n(H^+) dz} = A_S F(T) \frac{\int x(z) n^2(z) dz}{\int x^2(z) n^2(z) dz} = \frac{\mathcal{F}_2}{\mathcal{F}_3} A_S F(T).$$

Our GHRS absorption measurement gives $N(S^+)$ in the pencil beam to Mark 290. However, the [SII] emission measure is determined by the column density within the WHAM beam, which we estimate by scaling with the ratio of average $N(HI)$ in the WHAM beam to $N(HI)$ in the pencil beam to Mark 290. So:

$$A_S = \frac{y N(SII)}{N(H^+) + N(HI)_{WHAM}}, \text{ with } y = \frac{N(HI)_{WHAM}}{N(HI)_{Mark290}}.$$

We now have five equations for the seven unknowns T , $N(H^+)$, A_S , n_o , x_n , x_i and r , in terms of the observables $N(HI)_{WHAM}$, $N(HI)_{Mark290}$, α , $I(HII)$, $I([SII])$, $N(SII)$, and the distance. We can solve this system using the following procedure. First, assume a distance. Pick a value for T to calculate $EM(HII)$. Assume x_n and x_i , and solve for r , n_o and $N(H^+)$. From this calculate A_S and E . Iterate until the derived and observed values of E agree. Using the derived values of n_o and T , we can also calculate the pressure in the cloud as the product $n_o T$.

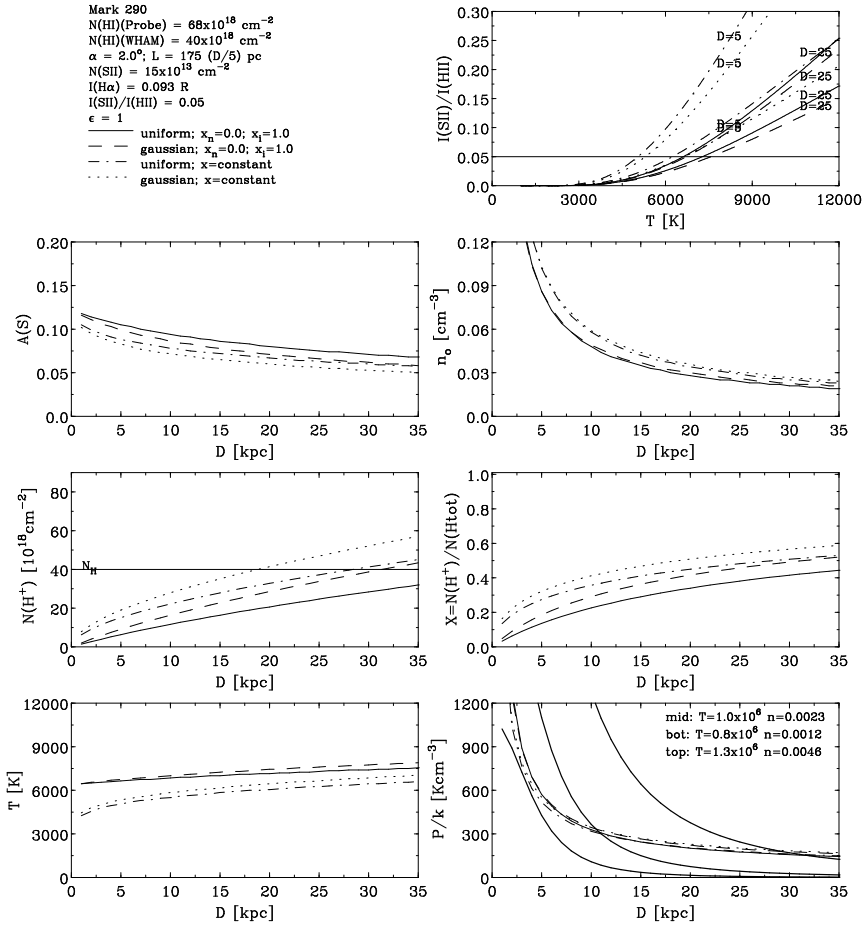


Figure 4. Derived values for gas temperature (T), S^+ abundance ($A(S)$), H^+ column density ($N(H^+)$), ionization fraction (X), central density (n_o) and central pressure (P), as a function of the unknown distance for four different geometries (as indicated in the upper left panel).

6. Physical conditions and metallicity - results

We now derive the metallicity and physical conditions inside complex C. We calculate a reference value using the following assumptions: a) the geometry is described by the “standard model” (constant density and a core-envelope ionization structure); b) all electrons come from H ($\epsilon=1$); c) 50% of the $H\alpha$ emission is associated with the -138 km/s component; d) $I([SII])/I(H\alpha)=1/20$; e) there is no saturation in the SII absorption; f) the SII absorption is only associated with the -138 km/s HI component; g) no fine structure correction is needed; h) a distance of 10 kpc.

With these assumptions, we can insert the observed values discussed in Sects. 3 and 4 into the system of equations discussed in Sect. 5 to find a sulphur abundance of 0.094 ± 0.020 times solar. Here we used a solar abundance

of 1.86×10^{-5} (Anders & Grevesse 1989). With only the Effelsberg HI data and the SII absorption column density we would have inferred an abundance of 0.121 ± 0.022 times solar.

The error we give here is just the statistical error associated with the measurements. It is dominated by the error in the SII column density. We now discuss the systematic errors introduced by the required assumptions.

A) Figure 4 shows the influence of four different assumptions for the geometry: a uniform or a gaussian density distribution in combination with either of two ionization structures: a neutral core and fully ionized envelope ($x_n=0$, $x_i=1$), or the same partial ionization throughout ($x_n=x_i=x$). Changing the density structure to a gaussian results in an abundance of 0.086, changing the ionization structure to constant partial ionization gives 0.078, changing both gives 0.072. So, the possible variation in the metallicity associated with geometry is $^{+0.000}_{-0.022}$. Of all uncertainties we discuss this is the only one that cannot easily be improved upon with better observations.

B) The assumption that all electrons come from hydrogen has little effect on the results: if in the fully-ionized region He were also fully ionized ($\epsilon \sim 1.14$), the derived abundance would be 0.097 (+0.003).

C) The $H\alpha$ emission is unresolved, so we cannot determine how much of the emission is associated with each HI component. If instead of 50%, 25% or 75% of the $H\alpha$ emission is associated with the -138 km/s component, the abundance changes by $^{+0.007}_{-0.005}$. A higher angular resolution $H\alpha$ spectrum can reduce this uncertainty.

D) We did not actually detect [SII] emission associated with complex C, but only have a (3σ) upper limit of $E = I([\text{SII}])/I(H\alpha) < 0.1$. A deeper observation of [SII] is being planned. For the sake of the calculation we assumed a value of 0.05. This uncertainty mostly influences the derived temperature. For E in the range 0.01–0.10, the derived sulphur abundance varies between 0.100 and 0.091, a range of $^{+0.006}_{-0.003}$.

E) If saturation is a problem for the SII absorption lines, the column density could be as high as $2.25 \times 10^{14} \text{ cm}^{-2}$, increasing the abundance by 0.046.

F) A major problem is posed by the fact that the HI spectrum shows two components, while only one is seen in the SII absorption spectrum. This problem could be solved by a higher S/N and higher resolution observation of the SII absorption. If we use the total HI column density of $111 \times 10^{18} \text{ cm}^{-2}$ (as well as the total $H\alpha$ emission), the derived abundance is 0.061 times solar, a change of -0.033 .

G) We do not yet know the precise value of HI toward Mark 290, as we used an Effelsberg spectrum with $9'$ beam. We will correct this to the value for a $1'$ beam using Westerbork observations. By comparing to similar cases (Wakker & Schwarz 1991, Lu et al. 1998) we expect a correction in the range 0.7–1.5. This changes the derived sulphur abundance to 0.137–0.062, a range of $^{+0.043}_{-0.032}$.

H) For an assumed range of distances from 5 to 25 kpc, the change in the derived metallicity is $^{+0.009}_{-0.019}$.

The ranges given above represent the largest deviations that can reasonably be expected, equivalent to a 3σ errorbar. To calculate a combined systematic error, we therefore add the ranges in quadrature and divide by 3. The sources of uncertainty can be split into three groups: those associated with physics (A–

E) $(^{+0.016}_{-0.008})$, those associated with the HI column density (F,G) $(^{+0.014}_{-0.015})$, and the uncertainty associated with the unknown distance (H) $(^{+0.003}_{-0.006})$. Combining these, the final value we derive for the sulphur abundance in complex C is $0.094 \pm 0.020^{+0.022}_{-0.019}$ times solar.

Figure 4 shows the dependence on the assumed geometry and distance for the derived parameters. Similar figures could be made showing the dependence on the other assumptions. As was the case for the abundance, we can derive a fiducial value and estimate the systematic error for the other parameters. We then find that: $X=0.23 \pm 0.06^{+0.07}_{-0.04}$, $n_o=0.048 \pm 0.010^{+0.011}_{-0.002}$ $(D/10)^{-0.5}$ cm $^{-3}$. $T=6800 \pm 500^{+750}_{-900}$ K, and $P=330 \pm 70^{+105}_{-45}$ $(D/10)^{-0.5}$ K cm $^{-3}$.

7. Discussion

7.1. Thermal pressure vs hot halo gas

We can compare the derived thermal pressure with the thermal pressure of hot halo gas. Wolfire et al. (1995) give a semi-empirical formula, using a base density for the hot gas $n(z=0)=0.0023$ cm $^{-3}$ and a temperature of order 10^6 K. From the ROSAT X-ray data, Snowden et al. (1998) find that the probable value of the halo temperature is $10^{6.02 \pm 0.08}$ K. The emission measure is about 0.02 cm $^{-6}$ pc (to within a factor of order 2), which for the density given above corresponds to a scaleheight of order 5 kpc. Such a scaleheight would be similar to that observed for the highly-ionized atoms of C $^{+3}$, N $^{+4}$ and O $^{+5}$ (Savage et al. 1997, Widmann et al. 1998).

The middle of the three bold-faced curves in the lower-right panel of Fig. 4 shows the semi-empirical relation for $n(z=0)=0.0023$ cm $^{-3}$, and $T=10^{6.02}$ K. Both the pressure relation derived by Wolfire et al. (1995) and the pressure derived by us represent the actual thermal pressure. Thus, if there is pressure equilibrium, the most likely values of $n(z=0)$ and T imply a distance to complex C of 10 kpc. If the hot halo temperature were $10^{5.94}$ K and the density were half as large, the implied distance is <3 kpc, incompatible with the observed lower limit. On the other hand, a higher temperature ($10^{6.10}$ K) and density (double the value) would result in equilibrium at a distance of 30 kpc. We conclude that for reasonable values for the density and temperature of hot halo gas, complex C cannot be more distant than ~ 30 kpc.

7.2. Mass, energy and mass flow

The mass of complex C can be calculated by summing the observed column densities, in the manner described by Wakker & van Woerden (1991). We make the assumptions that all the gas is at the same distance (unlikely, but we have insufficient information to justify a different assumption), that N(H₂) can be ignored (see Wakker et al. 1997), that N(H $^+$)/N(H_{tot})=0.23 everywhere, and that there is a 28% mass fraction of He. This yields a mass of $2.0 \times 10^6 (D/5 \text{ kpc})^2 M_\odot$.

To calculate the kinetic energy and mass flow associated with complex C requires some knowledge of its spatial velocity. Observed is the velocity relative to the LSR, which contains the motion of the Sun and a contribution from galactic rotation at the position of the object. To correct for these contributions we use the deviation velocity (Wakker 1991), the difference between the observed

LSR velocity and the maximum LSR velocity that can be easily understood in terms of differential galactic rotation. It is the minimum velocity that the cloud has relative to its local environment. Integrating the product of the mass and the square of the deviation velocity at each point in the cloud and correcting for H⁺ and He, leads to a kinetic energy of $>5.6 \times 10^{46} (D/5 \text{ kpc})^2 \text{ J}$, equivalent to the total energy of >500 supernovae.

We estimate the mass flow by making two different assumptions: A) the space velocity is completely radial ($v_z = v_{\text{dev}} \sin b$), or B) it is completely vertical ($v_z = v_{\text{dev}} / \sin b$). This gives 0.036 and 0.083 $(D/5 \text{ kpc}) M_{\odot} \text{ yr}^{-1}$, respectively. The area covered by complex C is 1623 square degrees ($12.4 (D/5 \text{ kpc})^2 \text{ kpc}^2$), so the corresponding infall rate is $2.9-6.7 \times 10^{-3} (D/5 \text{ kpc})^{-1} M_{\odot} \text{ yr}^{-1} \text{ kpc}^{-2}$. This value is similar to the rate of $\sim 4 \times 10^{-3} M_{\odot} \text{ kpc}^{-2} \text{ yr}^{-1}$ required by models of galactic chemical evolution (Giovagnoli & Tosi 1995). However, the theoretical rate should be present over the whole Galactic Disk, whereas the HVCs cover only $\sim 18\%$ of the sky. More HVC distances and metallicities are needed to solve this possible discrepancy.

7.3. Origins

Our metallicity excludes that complex C is part of a Galactic Fountain, as its metallicity then should have been >0.3 solar, the lowest value found in the outer galaxy (Afflerbach et al. 1997). The HVC thus must be extra-galactic.

Oort (1970) presented a model of continuing infall, in which gas originally near the (inhomogeneous) transition region separating Milky Way gas from intergalactic gas is still falling onto the Milky Way. This gas starts out hot and ionized, and becomes visible after interacting, cooling and mixing with high-z galactic gas associated with activity in the disk. Oort's model predicts z-heights of ~ 1 kpc and metallicities of ~ 0.7 times solar. The distance limits for HVC complexes A ($z=2.5-7$ kpc) and C ($z>3$ kpc) (van Woerden et al. 1998 and in these proceedings) and our metallicity result for complex C imply that the clouds would have to become neutral at much higher z than Oort's model suggests.

A Local Group origin for HVCs was first suggested by Verschuur (1969), who noted that according to the virial theorem some of the then-known clouds would be gravitationally stable at distances of 400 kpc. However, for most of the clouds found in later surveys the stability distance is several to tens of Mpc, implying $M \sim 10^{10} M_{\odot}$. Thus, this idea was no longer taken seriously. Blitz et al. (1998) point out that dark (and/or ionized) matter may be present, so that HI represents only 10–15% of the total mass. This reduces the average stability distance to 1 Mpc. Based on this and many other considerations, they suggest that the HVCs are remnants of the formation of the Local Group. The large HVCs, including complex C, would be nearby examples.

Extra-galactic HVCs could also represent gas orbiting the Milky Way, rather than gas in the Local Group at large. This was originally suggested by Kerr & Sullivan (1969), who considered HVCs to be loosely bound intergalactic material, too diffuse to contract into proto galaxies, orbiting the Galaxy at distances of order 50 kpc. They quote Toomre as suggesting that the source of this gas could be tidal streams pulled out of the Magellanic Clouds during previous passages. The metallicity would then be similar to that in the outer regions of the Magellanic Clouds >5 Gyr ago.

Mallouris et al. (1998) suggest that the HVCs are similar to Ly α absorbers. Vladilo (1998) suggests that damped Ly α absorbers are associated with dwarf galaxies. Therefore, low-metallicity HVCs such as complex C could be failed dwarf galaxies, in which in the early universe some of the gas formed stars, producing the observed metals, but where star formation has currently stopped.

References

Afflerbach A., Churchwell E., Werner M.W., 1997, ApJ, 478, 190
 Anders E., Grevesse N. 1989, Geoch. Cosmoch. Acta, 53, 197
 Beers T.C., Doinidis S.P., Griffin K.E., Preston G.W., Shectman S.A., 1992, AJ, 103, 267
 Beers T.C., Wilhelm R., Doinidis S.P., Mattson C.J., 1996, ApJS, 103, 433
 Blitz L., Spergel D., Teuben P., Hartmann D., Burton W.B., 1998, ApJ, in press
 Giovagnoli A., Tosi M., 1995, MNRAS, 273, 499
 Hartmann D., Burton W.B., 1997, *Atlas of Galactic Neutral Hydrogen*, (Cambridge: Univ. Press)
 Hulsbosch A.N.M., Wakker B.P., 1988, A&AS, 75, 191
 Kerr F.J., Sullivan III W.T., 1969, ApJ, 158, 115
 Lu L., Savage B., Sembach K., Wakker B., Sargent W., Oosterloo T., 1998, AJ, 115, 162
 Lucke P.B., 1978, A&A, 64, 367
 Mallouris C., York D.G., Lanzetta K., 1998, BAAS, 192, #51.09
 Oort J.H., 1970, A&A, 7, 381
 Preston G.W., Shectman S.A., Beers T.C., 1991, ApJ, 375, 121
 Reynolds R.J., Tufte S.L., Haffner L.M., Jaehnig K., Percival J.W., 1998, PASAu 15, 14
 Savage B.D., Sembach K.R., 1996, ARA&A, 34, 279
 Savage B.D., Sembach K.R., Lu L., 1997, AJ, 113, 2158
 Silk J., Wyse F.G., Shields G.A., 1987, ApJ, 322, L59
 Snowden S.L., Egger R., Finkbeiner D.P., Freyberg M.J., Plucinsky P.P., 1998, ApJ, 493, 715
 Verner D.A., Barthel P.D., Tytler D., 1994, A&AS, 108, 287
 Verschuur 1969, ApJ, 156, 771
 Vladilo G., 1998, ApJ, 493, 583
 Wakker B.P., 1991, A&A, 250, 499
 Wakker B.P., Murphy E.M., van Woerden H., Dame T.M., 1997, ApJ, 488, 216
 Wakker B.P., Schwarz U.J., 1991, A&A, 250, 484
 Wakker B.P., van Woerden H., 1991, A&A, 250, 509
 Wakker B.P., van Woerden H., Schwarz U.J., Peletier R.F., Douglas N.G., 1996, A&A, 306, L25
 Wakker B.P., van Woerden H., 1997, ARA&A, 35, 217

van Woerden H., Wakker B.P., Schwarz U.J., Peletier R.F., Kalberla P.M.W.,
1998, *Nature*, submitted

Widmann H., de Boer K., Richter P., Kramer G., Appenzeller I., Barnstedt J.,
Golz M., Grewing M., Gringel W., Mandel H., Werner K., 1998, *A&A*, 338,
L1

Wolfire M.G., McKee C.F., Hollenbach D., Tielens A., 1995, *ApJ*, 453, 673